Article

Pyrrolizidine Alkaloid Secondary Pyrrolic Metabolites Construct Multiple Activation Pathways Leading to DNA Adduct Formation and Potential Liver Tumor Initiation

Qingsu Xia, Xiaobo He, Liang Ma, Shoujun Chen, and Peter P. Fu

Chem. Res. Toxicol., **Just Accepted Manuscript** • DOI: 10.1021/acs.chemrestox.8b00096 • Publication Date (Web): 01 Jun 2018

Pyrrolizidine Alkaloid Secondary Pyrrolic Metabolites Construct Multiple Activation Pathways Leading to DNA Adduct Formation and Potential Liver Tumor Initiation

Qingsu Xia, Xiaobo He, Liang Ma, Shoujun Chen, and Peter P. Fu*

National Center for Toxicological Research, Food and Drug Administration, Jefferson, AR 72079, United States

* Corresponding Author: National Center for Toxicological Research, U.S. Food and Drug Administration, Jefferson, AR 72079, United States

Tel: +1-870-543-7207. Fax: +1-870-543-7136.
E-mail: peter.fu@fda.hhs.gov.

Table of Content

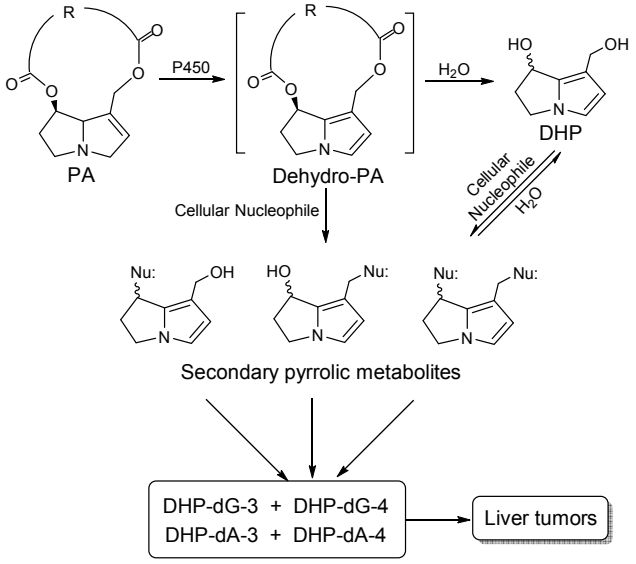

ABSTRACT

Pyrrolizidine alkaloids (PAs) and their *N*-oxide derivatives are hepatotoxic, genotoxic, and carcinogenic phytochemicals. PAs induce liver tumors through a general genotoxic mechanism mediated by a set of four (±)-6,7-dihydro-7-hydroxy-1-hydroxymethyl-5*H*-pyrrolizine (DHP)-derived DNA adducts. To date, the primary pyrrolic metabolites, dehydro-PAs, their hydrolyzed metabolite, DHP, and two secondary pyrrolic metabolites, 7-glutathione-DHP (7-GS-DHP) and 7-cysteine-DHP, are the known metabolites that can generate these DHP-DNA adducts *in vivo* and/or in PA-treated cells. Secondary pyrrolic metabolites are formed from the reaction of dehydro-PAs with glutathione, amino acids, and proteins. In this investigation, we determined whether or not more secondary pyrrolic metabolites can bind to calf thymus DNA and to cellular DNA in HepG2 cells resulting in the formation of DHP-DNA adducts by using a series of secondary pyrrolic metabolites (including 7-methoxy-DHP, 9-ethoxy-DHP, 9-valine-DHP, 7-GS-DHP, 7-cysteine-DHP, and 7,9-di-glutathione-DHP) and synthetic pyrroles for study. We found that: (i) many secondary pyrrolic metabolites are DNA reactive, can form DHP-DNA adducts; and (ii) multiple activation pathways are involved in producing DHP-DNA adducts associated with PA-induced liver tumor initiation. These results suggest that secondary pyrrolic metabolites play a vital role in the initiation of PA-induced liver tumors.

Keywords: Pyrrolizidine alkaloid; secondary pyrrolic metabolites; DHP; DHP-DNA adducts

INTRODUCTION

Pyrrolizidine alkaloids (PAs) and their *N*-oxides are phytochemicals present in thousands of plant species worldwide; with approximately half of these compounds are hepatototoxic, genotoxic, and tumorigenic.[1-12] Many herbal plants, herbal dietary supplements, and staple foods contain carcinogenic PAs and PA *N*-oxides.[2, 5, 7, 8, 10, 11, 13-17] It has been reported that a number of PAs and PA pyrrolic metabolites are able to induce tumors, particularly liver tumors, in rodents. Accordingly, the International Programme on Chemical Safety (IPCS) has concluded that PAs are a threat to human health and safety.[7] Monocrotaline, riddelliine, and lasiocarpine are classified as possible human carcinogens by the International Agency for Research on Cancer (IARC).[18, 19] The U.S. National Toxicology Program (NTP) listed riddelliine as "reasonably anticipated to be a human carcinogen" in the NTP 12th Report of Carcinogens in 2014.[20]

Upon metabolism, PAs and PA *N*-oxides generate primary pyrrolic reactive metabolites, dehydropyrrolizidine alkaloids (dehydro-PAs), which in the aqueous medium rapidly hydrolyze to (+/-)-6,7-dihydro-7-hydroxy-1-hydroxymethyl-5*H*-pyrrolizine (DHP).[2, 6, 8, 21] Dehydro-PAs and DHP are able to react with DNA, proteins, and amino acids resulting in forming DHP-DNA and DHP-protein adducts associated with cytotoxicity, genotoxicity, and carcinogenicity.[2, 3, 6, 8]

We recently determined that the metabolic activation of 12 tumorigenic PAs and PA *N*-oxides is by the identical biochemical mechanism, mediated by the formation of four DHP-DNA adducts (designated as DHP-dG-3, DHP-dG-4, DHP-dA-3, and DHP-dA-4) associated with liver tumor initiation (Figure 1).[3, 4, 22, 23] This set of DHP-DNA adducts has been formed in common, including (i) in the livers of rats dosed seven hepatocarcinogenic PAs (retrorsine, riddelliine, monocrotaline, lasiocarpine, heliotrine, clivorine, and senkirkine) and riddelliine *N*-oxide;[23] (ii) from the rat liver microsomal incubation of the *N*-oxides of riddelliine, retrorsine, monocrotaline, lasiocarpine, and heliotrine with calf thymus DNA;[22, 23] (iii) in the livers of male mice administered retrorsine;[24] and (iv) in the livers of cows accidently fed with hay containing PAs.[25] Consequently, we have proposed that these DHP-DNA adducts are biomarkers of PA and PA *N*-oxide exposure and PA-induced liver tumor initiation.[3, 22, 23, 26-28]

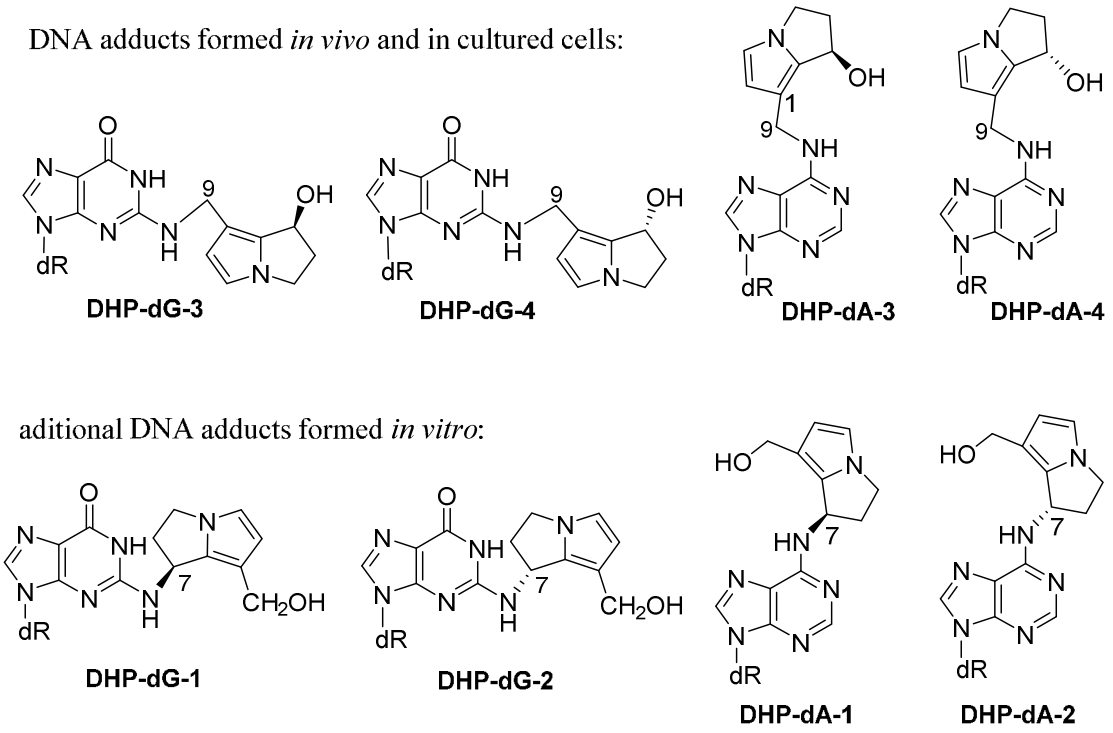

Figure 1. Structures of DHP-dG and DHP-dA adducts.

Dehydro-PAs are reactive bifunctional alkylating agents, capable of binding to DNA, proteins, amino acids, and glutathione at the nucleophilic sites carrying –OH, -NH, and the –SH functional groups. The resulting secondary pyrrolic metabolites, 7-substituted-DHP, 9-substituted-DHP, and 7,9-disubstituted-DHP themselves are reactive bifunctional alkylating agents as well, each possessing the oxygen-, nitrogen-, and/or sulfur-linkage at the C7 and/or C9 position.[8]

7-Glutathione-DHP (7-GS-DHP) and 7-cysteine-DHP are the known secondary pyrrolic metabolites that are formed from the reaction of dehydro-PAs with glutathione and cysteine, respectively.[27, 28] Very recently we found that 7-GS-DHP and 7-cysteine-DHP also produced this set of four DHP-DNA adducts by rat and human liver microsomes in the presence of calf thymus DNA and by incubation with human HepG2 cells.[3, 26-28] Based on these findings, we hypothesized that there could be more DNA reactive secondary pyrrolic metabolites.[3]

To pursue this goal, in the present study, eleven secondary pyrrolic metabolites and pyrroles, each of which possessing an O- (O-ethyl ether), an N- (N-ethyl ether), and/or an S- (thioether) linkage at C7 and/or C9 positions, were synthesized and used to determine their ability to produce DHP-DNA adducts from the reaction with calf thymus DNA and from incubation in HepG2 cells. The structures of the selected secondary pyrrolic metabolites and pyrroles are shown in Figure 2. These pyrrolic substrates include: (i) three 7-mono-substituted-DHPs: 1-hydroxymethyl-7-methoxy-6,7-dihydro-5-*H*-pyrrolizine (7-MeO-DHP), 7-GS-DHP, and 7-cysteine-DHP; (ii) two 9-mono-substituted-DHPs: 9-valine-DHP and 9-ethoxy-DHP (9-EtO-DHP); and (iii) six 7,9-di-substituted-DHPs: 7,9-di-valine-DHP, 7,9-di-MeO-DHP, 7,9-di-EtO-DHP, 7,9-di-GS-DHP, 7,9-di-cysteine-DHP, and 7,9-di-*N*-acetyl-cysteine-DHP (7,9-di-NAC-DHP). Among these substrates, 7-MeO-DHP is a known metabolite formed from the metabolism of senecionine by mouse liver microsomes.[29] Both 9-valine-DHP and 7,9-di-valine-DHP are metabolites formed from the human liver microsomal metabolism of monocrotaline in the presence of valine (results from this study). 7,9-Di-GS-DHP was formed from the metabolism of riddelliine by human liver microsomes in the presence of glutathione.[27] As described above, 7-GS-DHP and 7-cysteine-DHP have previously been studied. Dehydromonocrotaline and DHR (the 7-R enantiomer of the racemic DHP metabolite), which have been studied previously under similar experimental conditions, were included for comparison.[4, 23]

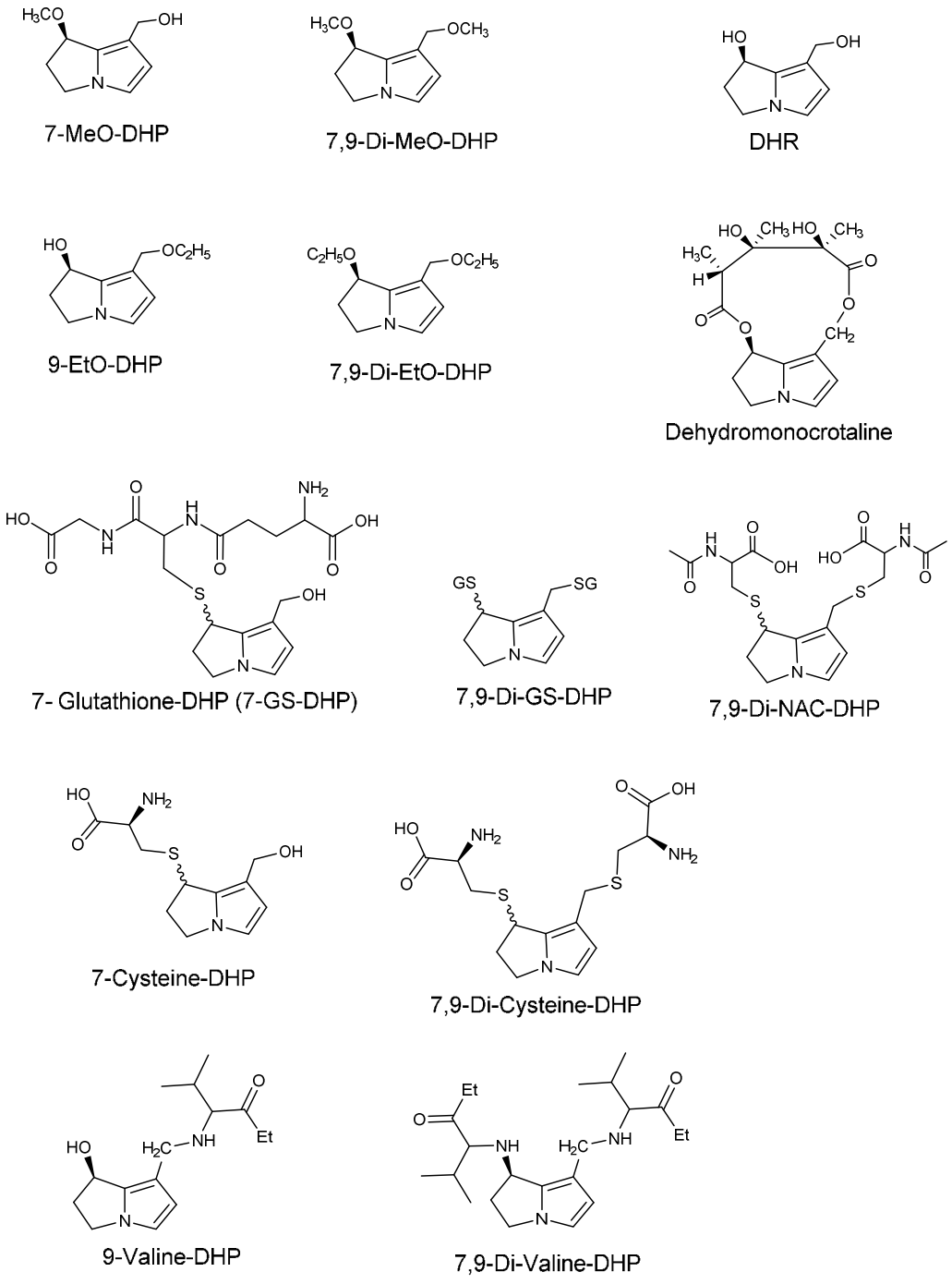

Figure 2. Structures of mono- and di-substituted secondary pyrrolic metabolites and pyrroles synthesized for this study.

EXPERIMENTAL PROCEDURES

Note: D*ehydromonocrotaline and DHR are carcinogens in laboratory animals and must be handled with safety precautions.*

Chemicals. Monocrotaline, glutathione (GSH), cysteine, *N*-acetylcysteine, calf thymus DNA, micrococcal nuclease (MN), nuclease P1, spleen phosphodiesterase (SPD), NADPH, 2'-deoxyguanosine (dG), and 2'-deoxyadenosine (dA) were obtained from Sigma-Aldrich (St. Louis, MO). Dimethylformamide (DMF), acetonitrile, potassium carbonate, chloroform, and diethyl ether were purchased from Fisher Scientific (Pittsburg, PA, USA). Absolute ethanol was purchased from AAPER Alcohol and Chemical Co (Shelbyville, KY). All solvents were LC/MS or HPLC grade. All DHP-DNA adducts (DHP-dG-1, DHP-dG-2, DHP-dG-3, DHP-dG-4, DHP-dA-1, DHP-dA-2, DHP-dA-3, and DHP-dA-4) and their isotope-labelled adducts (DHP-[$^{15}N_5$]dG-1, DHP-[$^{15}N_5$]dG-2, DHP-[$^{15}N_5$]dG-3, DHP-[$^{15}N_5$]dG-4, DHP-[$^{15}N_5$ $^{13}C_{10}$]dA-1, DHP-[$^{15}N_5$ $^{13}C_{10}$]dA-2, DHP-[$^{15}N_5$ $^{13}C_{10}$]dA-3, and DHP-[$^{15}N_5$ $^{13}C_{10}$]dA-4) were synthesized as described previously, and the purity of each was checked by HPLC before use.[4, 23, 30]

The human hepatocarcinoma HepG2 cell line was purchased from American Type Culture Collection (ATCC, Manassas, VA). Dulbecco's Modified Eagle's Medium (DMEM), fetal bovine serum (FBS), phosphate buffered saline (PBS, pH 7.4), trypsin-EDTA, penicillin, and streptomycin were purchased from Life Technologies (Grand Island, NY). Blood & Cell Culture DNA kits were purchased from QIAGEN (Valencia, CA). Mixed 50 Donor-pooled Human liver microsomes were purchased from Bioreclamation IVT (Baltimore, MD).

Dehydromonocrotaline and DHR were prepared from the reaction of monocrotaline and retronecine with *o*-chloroanil (or *o*-bromanil) in chloroform as described previously.[31, 32] 7-GS-DHP was synthesized and purified as previously described.[28, 33] 7,9-Di-glutathione-DHP (7,9-Di-GS-DHP) was similarly synthesized, with glutathione in a 5-fold excess,[28, 33] and was separated by HPLC (Phenomenex Luna C18 (2) column, 250 x 10 mm) using 20% methanol in water containing 0.1% formic acid with flow rate at 3 ml/min.[33]

7-Cysteine-DHP was prepared by reaction of cysteine in PBS (pH = 7.4) and dehydromonocrotaline in 2 mL DMF for 1 h followed by HPLC separation.[22] 7,9-Di-cysteine-

DHP was synthesized under similar experimental conditions, using cysteine in 5-fold excess.[22, 27] 7,9-Di-*N*-acetylcysteine (7,9-Di-NAC-DHP) was similarly prepared, with *N*-acetylcysteine (NAC) in a 7-fold excess.[28, 33]

Culvenor et al.[34] reported the synthesis of 7-MeO-DHP by reacting dehydroheliotridine (DHH), the enantiomer of DHR, with methanol under refluxing. In our study, reaction of DHR in methanol under refluxing overnight produced a mixture of 7-MeO-DHP, 9-MeO-DHP, and 7,9-di-MeO-DHP in 61.8, 7.8, and 6.8% yields, respectively. From the reaction mixture, 7-MeO-DHP was isolated by HPLC, with a C18 Prodigy column eluted with the following program: 0 – 5 min: 15% MeOH in H_2O; 5 – 45 min: 15 – 50% MeOH in H_2O at 1 mL/min. Reaction of DHR in methanol containing one drop of 2 N HCl with shaking for 2 min produced 7,9-di-MeO-DHP in near quantitative yield.

9-EtO-DHP was prepared by the reaction of absolute ethanol with dehydroheliotrine, which was synthesized by the reaction of heliotrine with *o*-chloroanil in chloroform, under experimental conditions similar to that for the synthesis of dehydromonocrotaline from monocrotaline.[32] The ^{1}H NMR spectrum of 9-EtO-DHP is shown in Figure S1 of Supporting Information. 7,9-Di-EtO-DHP was synthesized by reacting dehydromonocrotaline with ethanol at ambient temperature for 24 h following the method of [35] with modification.[36]

9-Valine-DHP was synthesized following the method we previously described[37] with modification. A mixture of 140 mg of valine (9.8 equiv of dehydromonocrotaline), 40 mg of K_2CO_3, 0.6 mL of distilled water, and 2.4 mL of DMF was added dropwise into a solution of 40 mg of dehydromonocrotaline in 3 mL of DMF. After reaction for 168 h, the mixture was separated by HPLC with a 250 × 10 mm Prodigy column (Phenomenex, Torrance, CA). The reaction products contained both 7-valine-DHP (previously assigned as DHP-valine-2 and DHP-valine-4) and 9-valine-DHP (previously assigned as DHP-valine-1 and DHP-valine-3).[37, 38] 9-Valine-DHP (DHP-valine-3) was collected for the present study. Di-valine-DHP was similarly prepared with a 20-fold excess of valine. The resulting product was separated by HPLC and characterized by mass and ^{1}H NMR spectral analyses. The full ^{1}H NMR spectral assignments of *7,9-di-valine-DHP* are: ^{1}H NMR (acetonitrile-d_3): δ 0.73 (3H, d, H7'/H8'/H15'/H16', J = 7 Hz), 0.85 (3H, d, H7'/H8'/H15'/H16', J = 7 Hz), 0.89 (3H, d, H7'/H8'/H15'/H16', J = 7 Hz), 1.05 (3H, d, H7'/H8'/ H15'/H16', J = 7 Hz), 1.17−1.20 (1H, m, H4'/H12'), 1.38−1.41 (1H, m, H12'/H4'), 2.38−2.45 (1H, m, H6b), 2.61−2.69 (1H, m, H6a), 3.59 (1H, d, H2'/H10', J = 3.3

Hz), 3.71 (1H, d, H10'/H2', J = 3.3 Hz), 3.78−3.84 (1H, m, H5b), 4.02−3.95 (1H, m, H5a), 4.16 (1H, H9b, dd, J = 14 Hz), 4.25 (1H, H9a, dd, J = 14 Hz), 5.70−5.76 (1H, m, H7), 6.10 (1H, d, H2, J = 2.5 Hz), 6.51 (1H, d, H3, J = 2.5 Hz).

Human Liver Microsomal Metabolism of Riddelliine in the Presence of Valine. The metabolism was conducted in a 1 mL incubation volume, consisting of 100 mM sodium phosphate buffer (pH 7.6), 1 mM NADPH, 5 mM $MgCl_2$, 500 μM riddelliine, 2 mM valine, and 1 mg of human liver microsomal protein at 37 °C for 1 h. After incubation, the incubation mixture was centrifuged at 105,000 g for 30 min at 4 °C and microsomal proteins removed, the supernatant was analyzed by LC-MS/MS.

Reaction of PA Pyrrolic Metabolites and Pyrroles with Calf Thymus DNA. A solution containing 0.5 mM 7-MeO-DHP and 1 mg calf thymus DNA in 1 mL acetonitrile and 0.01% formic acid water solution (pH 8 adjusted with ammonium hydroxide) at 1:1 volume was stirred at 37 °C for 72 h. The reaction mixture was then enzymatically hydrolyzed as previously described.[39] The resulting samples were spiked with internal standards DHP-[$^{15}N_5$]dGs and DHP-[$^{15}N_5$ $^{13}C_{10}$]dAs for LC-ESI/MS/MS analysis.

The reactions of vehicle control and other pyrroles were similarly conducted in parallel.

DHP-DNA Adducts Formed in Cultured HepG2 Cells Exposed to PA Pyrrolic Metabolites. Human HepG2 cells were cultured in DMEM supplemented with 10% (v/v) FBS and antibiotics (100 U/mL penicillin and 100 μg/mL streptomycin) at 37 °C in a humidified atmosphere containing 5% CO_2. One day before each experiment, cells were seeded at a density of 3×10^6 cell/mL in 150 cm^2 culture dishes. The cells were then exposed to vehicle control (0.1% DMSO in DMEM) and pyrrolic metabolites and analogs at 50 μM for 24 h.

After exposure, the cells were collected and DNA was extracted using a Blood & Cell Culture DNA Isolation kit following manufacturer's instructions. The concentration of the DNA was determined spectrophotometrically. DNA samples from treated or vehicle cells (200 μg) were then enzymatically hydrolyzed to nucleosides as described previously.[39]

Quantitation of DHP-dG and DHP-dA Adducts by LC/MS/MS Analysis. The LC/MS/MS identification and quantitation of the DHP-dG and DHP-dA adducts formed in each sample were conducted following the procedures previously published.[28]

Positive ions were acquired in the selected reaction monitoring (SRM) mode (dwell time of 100 ms). DHP-dG adducts were monitored at the $[M+H]^+$ *m/z* 403 to *m/z* 269 [M-H_2O+H-dR] transition;DHP-[$^{15}N_5$]dG internal standards at the $[M+H]^+$ *m/z* 408 to *m/z* 274 [M-H_2O+H-dR];DHP-dA adducts at the $[M+H]^+$ *m/z* 387 to *m/z* 253 [M-H_2O+H-dR]; DHP-[$^{15}N_5$ $^{13}C_{10}$]dA internal standards at the $[M+H]^+$ *m/z* 402 to *m/z* 263 [M-H_2O+H-dR] transition. Samples were quantified by comparing the areas of the unlabeled chromatogram peaks to those of the corresponding labeled internal standard chromatogram peaks. The Thermo Xcalibur 2.0 SR2 software was used for the data acquisition and reprocessing.

Standard characterization and calibration curves were obtained by plotting the amounts of standard compounds against peak area. In a 10 μL injection volume, each sample contained 40 fmol DHP-[$^{15}N_5$]dG and 10 fmol DHP-[$^{15}N_5$,$^{13}C_{10}$]dA.

Statistical Analysis. Assay data are presented as mean ± SD, the results represent two separate experiments conducted in triplicate. A two-sample t-test, assuming equal variances, in Excel was used to determine the significance between different treatments or doses. The difference was considered statistically significant when the p-value was less than 0.05.

RESULTS

Synthesis of Secondary Pyrrolic Metabolites and Pyrrole Analogs. Secondary pyrrolic metabolites and pyrrole analogs (Figure 2) used in this study were synthesized in our laboratory. Dehydromonocrotaline and DHR were the starting materials used for the synthesis of these secondary pyrrolic products. Because both dehydromonocrotaline and DHR are highly unstable, they had to be prepared in a highly pure form. These chemicals readily decomposed during reaction, resulting in erratic yields and difficulty in purification of the products by HPLC. The resulting pyrroles are reactive bifunctional alkylating agents, and are also highly unstable and easily decomposed. For example, 7,9-di-EtO-DHP in acetonitrile decomposed into 7-EtO-DHP and 9-EtO-DHP even when stored at -80 ºC. Consequently, all these substrates had to be

synthesized a highly pure form; and after storage, had to be purified again before use. For illustration, the dehydromonocrotaline that we prepared is highly pure, as demonstrated by its ^{1}H NMR shown in Figure S2 of Supporting Information.

Human Liver Microsomal Metabolism of Riddelliine in the Presence of Valine. After the metabolism, 9-valine-DHP and 7,9-di-valine-DHP were identified based on comparing their HPLC retention times, UV-visible absorption spectra, and mass spectra with those of the synthetic standards. The formation of these two metabolites was further confirmed by comparison of their LC/MS/MS selected reaction monitoring (SRM) mode profiles (Figure S3 of Supporting Information) with those of the synthetic standards.

Standard Characterization and Calibration Curves. HPLC-ES-MS/MS calibration curves were obtained from DHP-dGs and DHP-dAs versus their respective isotope-labelled (Figures S4 and S5 of Supporting Information).

Reactions of Pyrrolic Metabolites and Pyrroles with Calf Thymus DNA. DNA samples isolated from each reaction were enzymatically hydrolyzed to nucleosides from which the DHP-dG and DHP-dA adducts were quantified.

The quantitation of these adducts formed from each reaction are summarized in Table 1. LC/MS/MS SRM chromatograms of DHP-dG and DHP-dA adducts generated from the reaction of calf thymus DNA with vehicle control (solvent) and with 7-MeO-DHP are shown in Figure 3A and Figure 3B, respectively. Figure 3A-1 and Figure 3B-1 show the isotope-labeled internal standards DHP-[$^{15}N_5$]dG-1, DHP-[$^{15}N_5$]dG-2, DHP-[$^{15}N_5$]dG-3, and DHP-[$^{15}N_5$]dG-4 adducts, each involving the transition of the $[M+H]^+$ precursor ion *m/z* 408 to the selected product ion *m/z* 274. Figure 3A-3 and Figure 3B-3 are DHP-[$^{15}N_5$, $^{13}C_{10}$]dA-1, DHP-[$^{15}N_5$,$^{13}C_{10}$]dA-2, DHP-[$^{15}N_5$,$^{13}C_{10}$]dA-3, and DHP-[$^{15}N_5$,$^{13}C_{10}$]dA-4 adducts involving the transition of *m/z* 402 to *m/z* 263. Figure 3A-2 and Figure 3A-4 present the DHP-dG and DHP-dA adducts formed from the control, which indicate that these DHP-dG and DHP-dA adducts were not detected (Table 1). The results shown in Figure 3B-2 and Figure 3B-4 indicate that the reaction of 7-MeO-DHP with calf thymus DNA generated all the four DHP-dG and four DHP-dA adducts and that the total level of DHP-dG adducts are higher than those of DHP-dA adducts (Table 1).

SRM chromatograms from reactions of 7-valine-DHP and 7,9-di-valine-DHP with calf thymus DNA for 72 h are shown in Figure 4. All the four DHP-dG and four DHP-dA adducts

were generated from both 7-valine-DHP and 7,9-di-valine-DHP. Also, the level of DHP-dG adducts formation was higher than that of DHP-dA adducts (Table 1).

As summarized in Table 1, the eleven secondary pyrrolic metabolites and pyrrolic analogs, together with dehydromonocrotaline and DHR, all generated the four DHP-dG adducts and the four DHP-dA adducts. With the exceptions of 7,9-di-GS-DHP, 7,9-di-cysteine-DHP, and 7,9-di-NAC-DHP, all the compounds produced high levels of DHP-DNA adducts. The levels of DHP-dG-3/4 adducts were significantly higher than those of DHP-dA-3/4 adducts. 7,9-Di-GS-DHP, 7,9-di-cysteine-DHP, and 7,9-di-NAC-DHP produced much lower levels of DHP-DNA adducts. No DHP-dG or DHP-dA adducts were detected from the vehicle control group.

Table 1. LC-MS/MS Measurements of DHP-dG and DHP-dA Adducts Formed from Reaction of Mono- and Di-Substituted Pyrrolic Metabolites and Analogs with Calf Thymus DNA for 72 Hours.

Chemicals	Levels of DHP-dG and DHP-dA / 10^8 nucleosides[c]						
	DHP-dG-1	DHP-dG-2	DHP-dG-3/4	DHP-dA-1	DHP-dA-2	DHP-dA-3/4	Total DHP-dG and DHP-dA
Vehicle Control	<LOD[d]	<LOD	<LOD	<LOD	<LOD	<LOD	<LOD
7,9-Di-EtO-DHP[a]	16010 ± 1495	13220 ± 1722	16193 ± 1718	2830 ± 126	1955 ± 146	3499 ± 271	53707
9-EtO-DHP[a]	16740 ± 1382	13768 ± 1419	20022 ± 1759	4282 ± 328	2925 ± 349	4610 ± 395	62346
7,9-Di-MeO-DHP[a]	15029 ± 703	13046 ± 251	15715 ± 510	2736 ± 108	1949 ± 32	3110 ±91	51586
7-MeO-DHP[a]	6036 ± 434	5325 ± 398	9409 ± 570	1335 ± 198	1050 ± 166	2717 ± 300	25872
7,9-Di-Valine-DHP[a]	9847 ± 1201	5051 ± 542	11525 ± 1372	1583 ± 226	1510 ± 145	5516 ± 370	35032
9-Valine-DHP[a]	10977 ± 988	5762 ± 630	26040 ± 1679	1947 ± 170	1823 ± 168	5804 ± 500	52354
7-GS-DHP	16948 ± 929	13982 ± 723	26220 ± 1146	6064 ± 417	3950 ± 422	8006 ± 382	75169
7-Cysteine	19326 ± 1034	14769 ± 714	33443 ± 1238	7059 ± 392	4604 ± 487	9313 ± 554	88514
7,9-Di-GS-DHP[b]	8.2 ± 0.8	2.7 ± 0.3	12.0 ± 0.7	2.2 ± 0.4	2.0 ± 0.2	14.3 ± 1.3	41.5
7,9-Di-cysteine-DHP[b]	11.3 ± 0.8	6.7 ± 0.7	17.1 ± 1.5	3.5 ± 0.3	3.0 ± 0.2	10.7 ± 1.0	52.4
7,9-Di-NAC-DHP[b]	16.2 ± 1.5	17.7 ± 1.6	22.0 ± 2.0	8.0 ± 0.6	3.5 ± 0.2	11.5 ± 0.8	78.8
DHR[a]	13859 ± 1476	11433 ± 960	25529 ± 1819	5478 ± 490	3771 ± 366	7039 ± 446	67109

Dehydromonocrotaline[a]	12363 ± 1065	10285 ± 1110	21043 ± 1538	4034 ± 331	3063 ± 219	6915 ± 523	57703

[a] Aliquots of DNA (0.13 µg) were assayed by HPLC-ES-MS/MS. [b] Aliquots of DNA (39.6 µg) were assayed by HPLC-ES-MS/MS. [c]The data are presented as the mean ± SD, n=3. [d]LOD = limit of detection based upon the analysis of 45 µg DNA by HPLC-ES-MS/MS. Under experimental conditions, the LOD of DHP-dG-1/2 is 0.71, DHP-dG-3/4 is 0.71, DHP-dA-1/2 is 0.14, and DHP-dA-3/4 is 0.14 adducts per 10^8 nucleosides, separately.

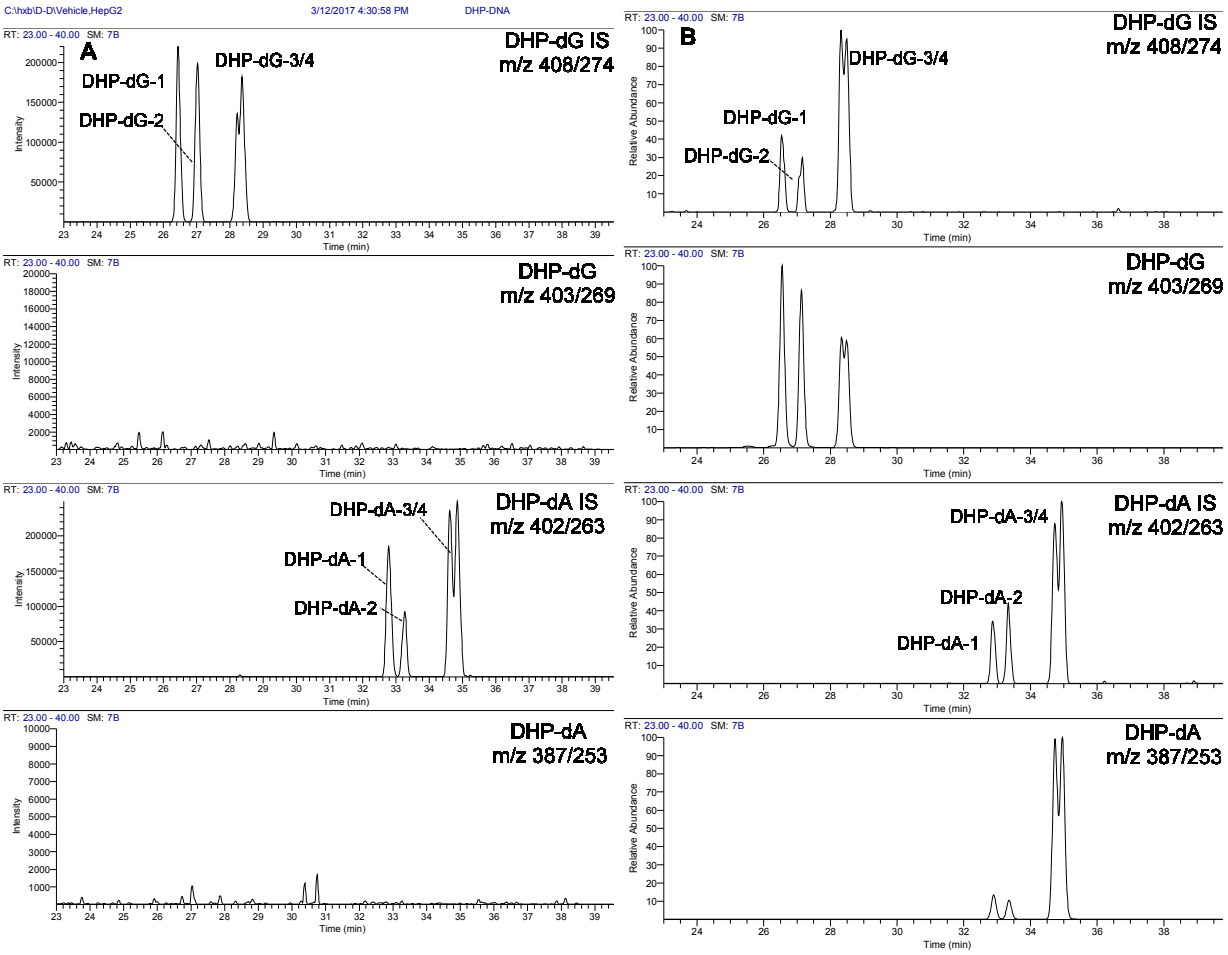

Figure 3. LC/MS/MS SRM chromatograms of DHP-dG and DHP-dA adducts formed from (A) vehicle control; and (B) reaction of 50 µM 7-MeO-DHP with calf thymus DNA for 72 h. IS: DHP-[$^{15}N_5$]dG and DHP-[$^{15}N_5$,$^{13}C_{10}$]dA labeled internal standards.

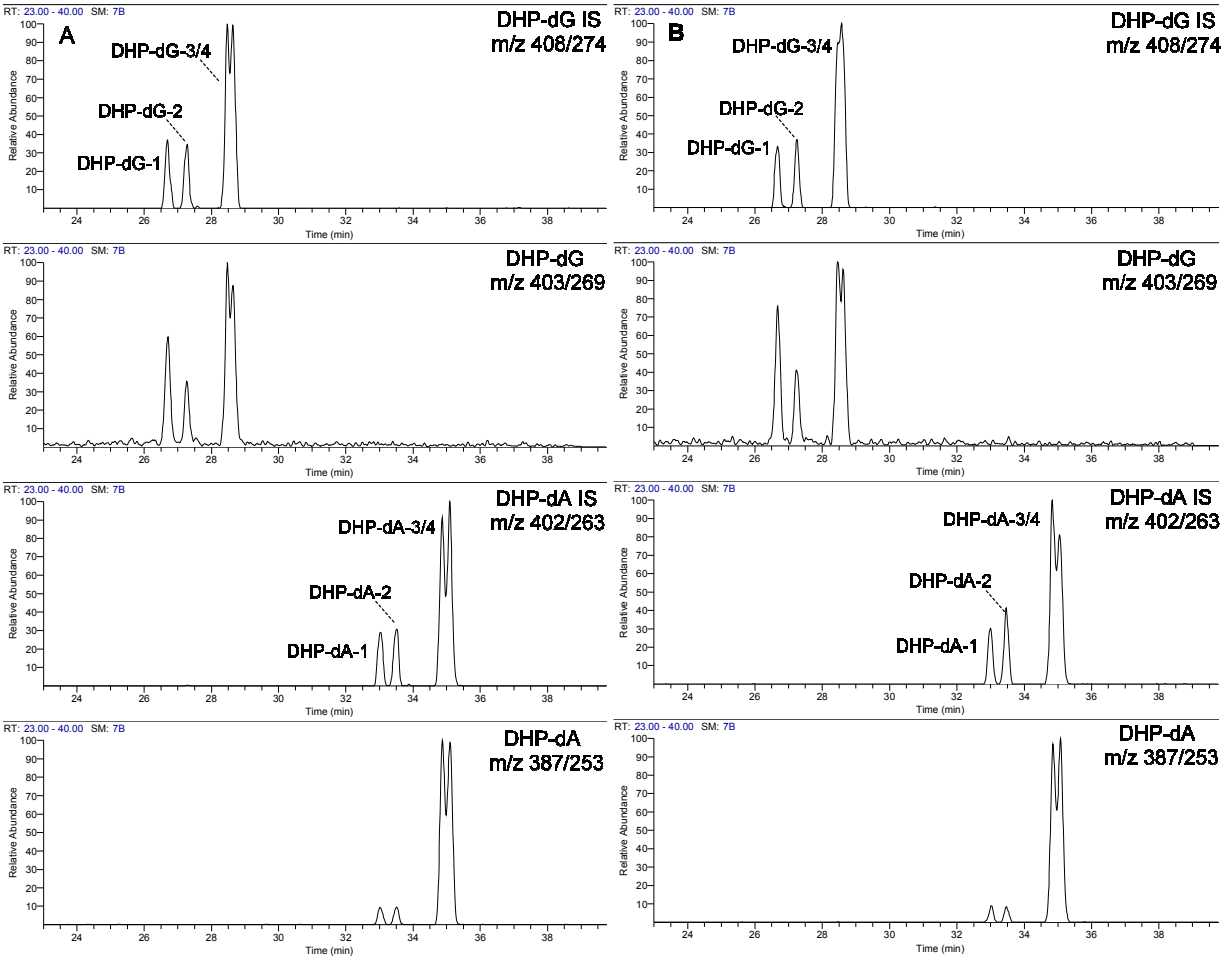

Figure 4. LC/MS/MS SRM chromatograms of DHP-dG and DHP-dA adducts formed from reaction of (A) 50 μM 9-valine-DHP and (B) 7,9-di-valine-DHP with calf thymus DNA for 72 h.

LC-MS/MS Analysis of DHP-dG and DHP-dA Adducts in HepG2 Cells Exposed to Mono- and Di-Substituted Pyrrolic Metabolites. The levels of DHP-dG and DHP-dA adducts formed in HepG2 cells treated with individual pyrrolic metabolites and pyrrolic analogs are summarized in Table 2. As examples, LC/MS/MS SRM chromatograms of DHP-dG and DHP-dA adducts formed from HepG2 cells exposed to 50 μM of 7-valine-DHP (Figure 5-A) and 7,9-di-valine-DHP (Figure 5-B) for 24 h are shown in Figure 5.

Compared with the results from the reaction with calf thymus DNA (Table 1), only DHP-dG-3/4 and DHP-dA-3/4 adducts were formed; DHP-dG-1, DHP-dG-2, DHP-dA-1, and DHP-dA-2 were not detected (Table 2). This DHP-DNA adduct pattern corresponds to that observed *in vivo*

[3, 4, 23]. The levels of DHP-dA-3/4 adducts were lower than those of DHP-dG-3/4 adducts. No DHP-dG or DHP-dA adducts were detected from the control incubations. No DHP-DNA adducts were detected in the HepG2 cells treated with 7,9-di-GS-DHP, 7,9-di-cysteine-DHP, or 7,9-di-NAC-DHP.

Table 2. LC-MS/MS Analysis of DHP-dG and DHP-dA Adducts for HepG2 Cells Exposed to Mono- and Di-Substituted Pyrrolic Metabolites and Analogs at 50 μM for 24 hours.

Chemicals	**Levels of DHP-dG and DHP-dA / 10^8 nucleosides[a]**						
	DHP-dG-1	DHP-dG-2	DHP-dG-3/4	DHP-dA-1	DHP-dA-2	DHP-dA-3/4	Total DHP-dG and DHP-dA
Control incubation	<LOD	<LOD	<LOD	<LOD	<LOD	<LOD	<LOD
7,9-di-EtO-DHP	<LOD	<LOD	1.3 ±0.3	<LOD	<LOD	0.4 ± 0.1	1.7
9-EtO-DHP	<LOD	<LOD	12.3 ±1.1	<LOD	<LOD	2.3 ± 0.3	14.6
7,9-di-MeO-DHP	<LOD	<LOD	2.3 ± 0.4	<LOD	<LOD	0.6 ± 0.1	2.9
7-MeO-DHP	<LOD	<LOD	4.0 ± 0.3	<LOD	<LOD	0.8 ± 0.1	4.8
7,9-di-Valine-DHP	<LOD	<LOD	4.1 ± 0.5	<LOD	<LOD	0.8 ± 0.1	4.9
7-Valine-DHP	<LOD	<LOD	8.4 ± 1.0	<LOD	<LOD	1.4 ± 0.2	9.8
7-GS-DHP	<LOD	<LOD	10.0 ± 1.0	<LOD	<LOD	1.7 ± 0.1	11.7
7-cysteine-DHP	<LOD	<LOD	11.4 ± 1.4	<LOD	<LOD	2.0 ± 0.2	13.4
7,9-di-GS-DHP	<LOD	<LOD	<LOD	<LOD	<LOD	<LOD	<LOD
7,9-di-cysteine-DHP	<LOD	<LOD	<LOD	<LOD	<LOD	<LOD	<LOD
7,9-di-NAC-DHP	<LOD	<LOD	<LOD	<LOD	<LOD	<LOD	<LOD
DHR	<LOD	<LOD	6.6 ± 0.7	<LOD	<LOD	1.2 ± 0.1	7.8
Dehydromonocrotaline	<LOD	<LOD	11.3 ± 1.2	<LOD	<LOD	1.9 ± 0.2	13.2

[a]Aliquots of DNA (45 μg) were assayed by HPLC-ES-MS/MS. The data are presented as the mean ± SD, n=3. [b]The LOD values are identical to those described in the note of Table 1.

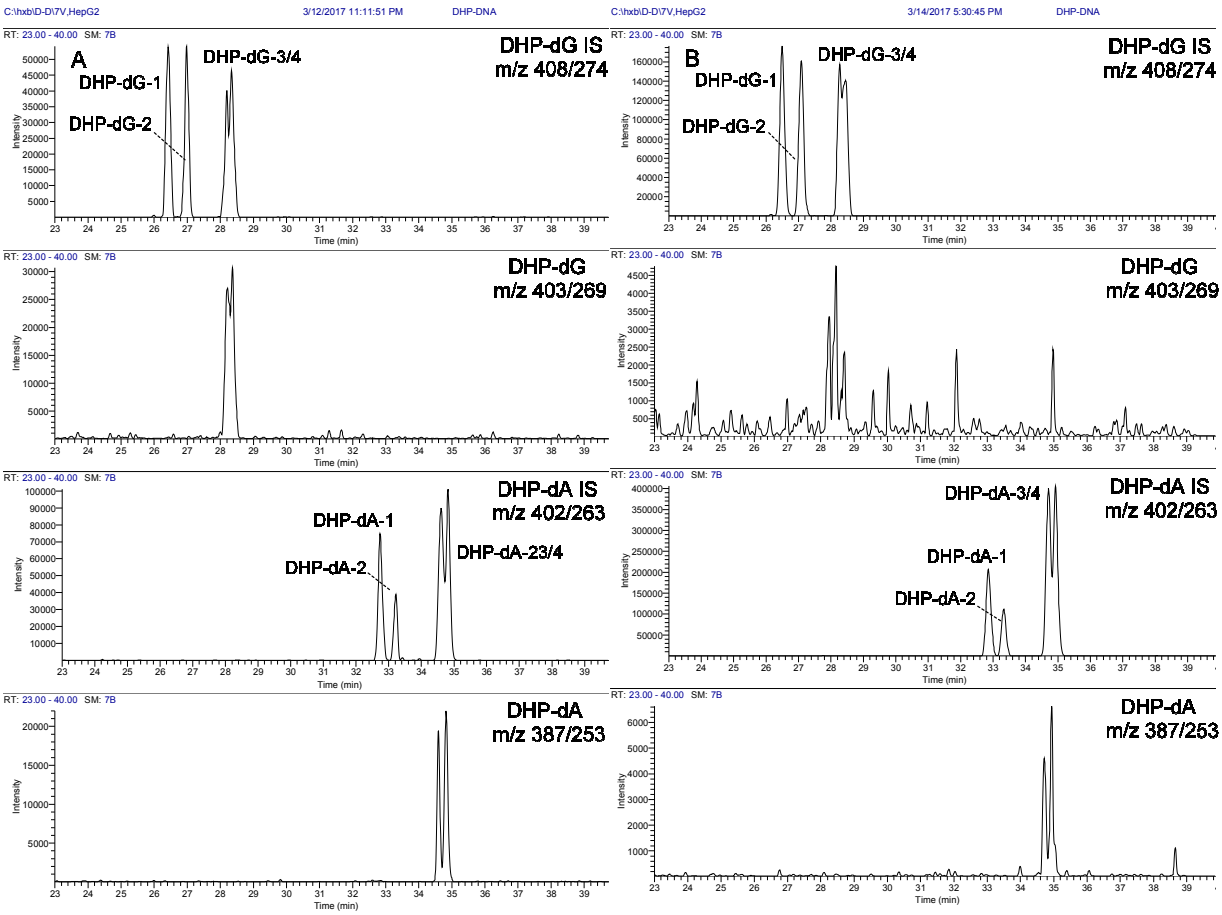

Figure 5. LC/MS/MS SRM chromatograms of DHP-dG and DHP-dA adducts formed from HepG2 cells exposed to (A) 50 μM 9-valine-DHP and (B) 7,9-di-valine-DHP for 24 h.

DISCUSSION

We proposed that DHP-DNA adducts are biomarkers of PA exposure and PA-induced liver tumor initiation. To validate this hypothesis and determine if additional metabolites can generate these DHP-DNA adducts, the ability of 13 secondary pyrrolic metabolites and pyrrolic analogs to bind calf thymus DNA and cellular DNA in HepG2 cells was studied. We found that all these secondary pyrroles can bind to calf thymus DNA and produce the same set of DHP-DNA adducts (Table 1).

When incubated with HepG2 cells, with the exception that no DHP-DNA adducts were detected from the 7,9-di-GS-DHP, 7,9-di-cysteine-DHP, and 7,9-di-NAC-DHP groups, the

remaining 10 pyrroles generated these DHP-DNA adducts (DHP-dG-3, DHP-dG-4, DHP-dA-3, and DHP-dA-4 adducts) (Table 2). The DNA adduct profile obtained from these secondary pyrrolic metabolites is similar to that produced in the livers of rats, mice, and cattle *in vivo*.[3, 4, 23, 24] The uniqueness of this profile is that: (i) no DHP-dG-1, DHP-dG-2, DHP-dA-1, and DHP-dA-2 were detected; and (ii) the levels of DHP-dG-3/4 adduct formation were significantly higher than those of DHP-dA-3/4 adducts (Table 2).

In this study all secondary pyrroles possess an O-ether linkage, an *N*-secondary amine linkage, or a thioether-linkage located at the C7 and/or C9 position of the necine base (Figure 2). Removal of the O-, S-, or *N*-substituent produces carbonium ions located at the C7 or C9 position that can be stabilized by resonance with the π-electrons at the two conjugated double bonds and the nitrogen atom of the necine base.[8] These carbonium ions bind to other nucleophiles producing new alkylated-DHP products. When the attacked nucleophile is DNA, the resulting alkylated DHP products are DHP-DNA adducts. Based on the results obtained in this present study, many secondary pyrrolic metabolites, which are produced from the reactions of dehydro-PAs with glutathione, amino acids, and proteins, are able to produce DHP-DNA adducts through the reaction with DNA. [2, 8, 22, 27, 28, 40, 41] Consequently, there are multiple activation pathways that result in the formation of DHP-DNA adducts associated with PA-induced liver tumor initiation. Based on these findings, we propose a general multiple metabolic activation pathway (Figure 6) to mediate the formation of these DHP-DNA adducts. Dehydro-PAs are highly unstable[8, 42] while the secondary pyrrolic metabolites are relatively more stable.[8] In consideration of this fact, secondary pyrrolic metabolites should play a vital role in the PA-induced liver tumor initiation.

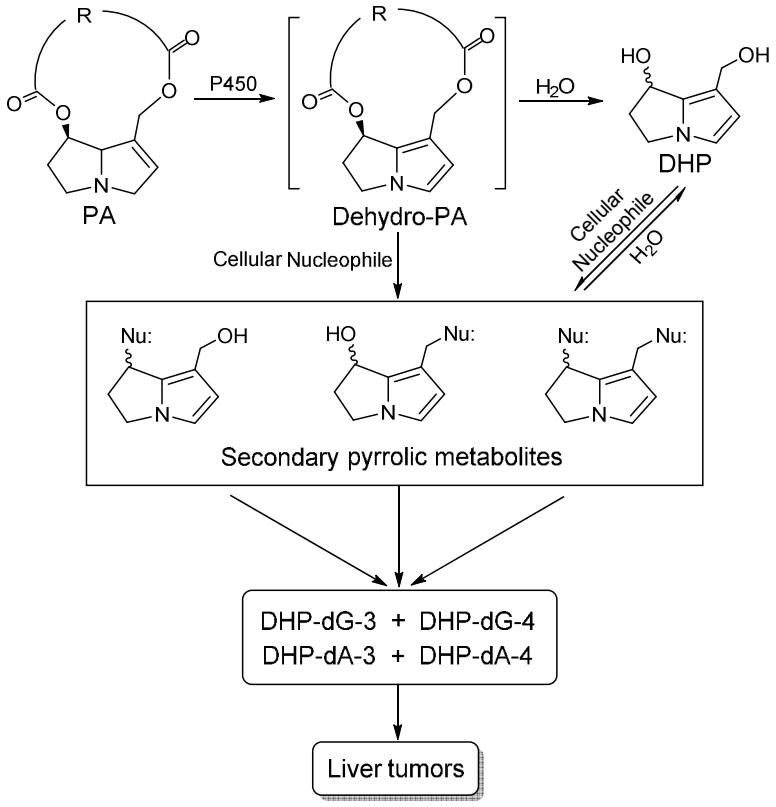

Figure 6. Proposed PA secondary pyrrolic metabolites construct multiple activation pathways leading to DNA adduct formation and potential liver tumor initiation.

Among the three atoms, oxygen has the highest electronegativity (3.44), possessing the most electron attracting ability. As such, oxygen attracts electrons easier than the nitrogen atom, which has an electronegativity number 3.04, and much easier than the sulfur atom which has a lower electronegativity number (2.58). Consequently, the –O-ether linkage at the C7 or C9-position of a pyrrole is most unstable, followed by the N-ether-linkage, and –S-linkage is most stable. Based on our experience in handling these compounds, we have found that 7-GS-DHP and 7-cysteine-DP are more stable than 9-valine-DHP, 7-MeO-DHP, and 9-EtO-DHP. These observations are in agreement with the report by Mattocks[8] that stated "those the nucleophile bound to the DHP moiety through a sulfuhydryl linkage are more stable than those linked by an oxygen atom or a nitrogen atom".

It has been well established that the reaction of pyrrolic metabolites with nucleophilic cellular substituents is an SN1 type mechanism,[4, 8] mediated by the formation of an oxygenium ion, an nitronium ion, or a sulfonium ion. In order to produce DHP-DNA adducts, 7,9-di-GS-DHP, 7,9-di-cysteine-DHP, and 7,9-di-NAC-DHP need to remove two sulfonium ions, and the removal of the first sulfonium ion should be the rate-determining step. Consequently, 7,9-di-GS-DHP, 7,9-di-cysteine-DHP, and 7,9-di-NAC-DHP exhibit low or non-binding activity in the production of DHP-DNA adducts (Tables 1 and 2), while 7,9-di-MeO-DHP, 7,9-di-EtO-DHP, and 7,9-di-valine-DHP can bind to DNA.

The results obtained in this present study indicate that the set of DHP-DNA adducts (DHP-dG-3, DHP-dG-4, DHP-dA-3, and DHP-dA-4) could be generated through the binding of a variety of metabolism products, including: (i) primary pyrrolic metabolites; (ii) secondary pyrrolic metabolites; and (iii) DHP-protein adducts. If this is the case, these DHP-DNA adducts provide useful common biomarkers of PA exposure and PA-induced liver tumor initiation. This warrants further investigation.

Concerning the study of the metabolic activation of chemical carcinogens, our findings represent the first case that a series of reactive secondary pyrrolic metabolites are generated of which some are expected to form DNA adducts in inducing mutations leading to liver tumorigenesis.

ASSOCIATED CONTENT

Supporting Information

Figures S1−S2 show the NMR spectra of the synthesized 9-EtO-DHP, monocrotaline, and dehydromonocrotaline. Figures S3 are the LC/MS SRM chromatograms of mono-valine-DHP and 7,9-di-valine-DHP, and Figures S4−S5 show the standard characterization and calibration curves of DHP-DNA adducts. This material is available free of charge via the Internet at http://pubs.acs.org.

AUTHOR INFORMATION

Funding

This research was supported in part by appointment (X.H.) to the Postgraduate Research Program at the NCTR administered by the Oak Ridge Institute for Science and Education through an interagency agreement between the U.S. Department of Energy and the FDA.

Qingsu Xia and Xiaobo He equally contribute the work and share the first authorship.

ACKNOWLEDGMENTS

We thank Drs. Frederick A. Beland and Danial R. Doerge for critical review of this manuscript. This article is not an official U.S. FDA guidance or policy statement. No official support or endorsement by the U.S. FDA is intended or should be inferred. The authors declare no competing financial interest.

ABBREVIATIONS

DMF, dimethylformamide; DHR, dehydroretronecine or (-)-R-6,7-dihydro-7-hydroxy-1-hydroxymethyl-5*H*-pyrrolizine; DHP, (+/-)-6,7-dihydro-7-hydroxy-1-hydroxymethyl-5*H*-pyrrolizine; 7-GS-DHP, 7-glutathione-DHP; 7,9-di-GS-DHP, 7,9-diglutathione-DHP; NAC, *N*-acetylcysteine; PNK, cloned T4 polynucleotide kinase; MN, micrococcal nuclease; SPD, spleen phosphodiesterase; dG, 2'-deoxyguanosine; dA, 2'-deoxyadenosine; DHP-dG-1 and DHP-dG-2, a pair of epimers of 7-(deoxyguanosin-N^2-yl)dehydrosupinidine adducts; DHP-dG-3 and DHP-dG-4, a pair of epimers of 7-hydroxy-9-(deoxyguanosin-N^2-yl)dehydrosupinidine adducts; DHP-dA-1 and DHP-dA-2, a pair of epimers of 7-(deoxyadenosin-N^6-yl)dehydrosupinidine adducts; DHP-dA-3 and DHP-dA-4, a pair of epimers of 7-hydroxy-9-(deoxyadenosin-N^6-yl)dehydrosupinidine adducts; LC-ES-MS/MS, high-performance liquid chromatography electrospray ionization tandem mass spectrometry; SRM, selected reaction monitoring; LOD, limit of detection; NCTR, National Center for Toxicological Research.

REFERENCES

(1) Cook, J. W., Duffy, E., and Schoental, R. (1950) Primary liver tumours in rats following feeding with alkaloids of Senecio jacobaea. *Br. J. Cancer 4*, 405-410.

(2) Edgar, J. A., Molyneux, R. J., and Colegate, S. M. (2015) Pyrrolizidine alkaloids: potential role in the etiology of cancers, pulmonary hypertension, congenital anomalies, and liver disease. *Chem. Res. Toxicol. 28*, 4-20.

(3) Fu, P. P. (2017) Pyrrolizidine Alkaloids: Metabolic activation pathways leading to liver tumor initiation. *Chem. Res. Toxicol. 30*, 81-93.

(4) Fu, P. P., Chou, M. W., Churchwell, M., Wang, Y., Zhao, Y., Xia, Q., Gamboa da Costa, G., Marques, M. M., Beland, F. A., and Doerge, D. R. (2010) High-performance liquid chromatography electrospray ionization tandem mass spectrometry for the detection and quantitation of pyrrolizidine alkaloid-derived DNA adducts *in vitro* and *in vivo*. *Chem. Res. Toxicol. 23*, 637-652.

(5) Fu, P. P., Chou, M. W., Xia, Q., Yang, Y.-C., Yan, J., Doerge, D. R., and Chan, P. C. (2001) Genotoxic pyrrolizidine alkaloids and pyrrolizidine alkaloid *N*-oxides—mechanisms leading to DNA adduct formation and tumorigenicity. *J. Environ. Sci. Health, Part C 19*, 353-385.

(6) Fu, P. P., Xia, Q., Lin, G., and Chou, M. W. (2004) Pyrrolizidine alkaloids--genotoxicity, metabolism enzymes, metabolic activation, and mechanisms. *Drug Metab. Rev. 36*, 1-55.

(7) IPCS. (1989) Pyrrolizidine Alkaloids Health and Safety Guide, In *Health and Safety Criteria Guide 26.* p p.19, International Programme on Chemical Safety, WHO: Geneva, Switzerland.

(8) Mattocks, A. R. (1986) *Chemistry and Toxicology of Pyrrolizidine Alkaloids.*, Academic Press, London, NY.

(9) Peterson, J. E., Jago, M. V., Reddy, J. K., and Jarrett, R. G. (1983) Neoplasia and chronic disease associated with the prolonged administration of dehydroheliotridine to rats. *J. Natl. Cancer Inst. 70*, 381-386.

(10) Roeder, E. (2000) Medicinal plants in China containing pyrrolizidine alkaloids. *Pharmazie 55*, 711-726.

(11) Roeder, E. (1995) Medicinal plants in Europe containing pyrrolizidine alkaloids. *Pharmazie 50*, 83-98.

(12) Xia, Q., Chou, M. W., Kadlubar, F. F., Chan, P.-C., and Fu, P. P. (2003) Human liver microsomal metabolism and DNA adduct formation of the tumorigenic pyrrolizidine alkaloid, riddelliine. *Chem. Res. Toxicol. 16*, 66-73.

(13) Bodi, D., Ronczka, S., Gottschalk, C., Behr, N., Skibba, A., Wagner, M., Lahrssen-Wiederholt, M., Preiss-Weigert, A., and These, A. (2014) Determination of pyrrolizidine alkaloids in tea, herbal drugs and honey. *Food add. contam. Part A, Chem, anal, control, expo. risk assess.t 31*, 1884-1895.

(14) Edgar, J. A., Lin, H. J., Kumana, C. R., and Ng, M. M. (1992) Pyrrolizidine alkaloid composition of three Chinese medicinal herbs, Eupatorium cannabinum, E. japonicum and Crotalaria assamica. *Am. J. Chin. Med. 20*, 281-288.

(15) Fu, P. P., and Xia, Q. (2015) Pyrrolizidine alkaloids: toxic phytochemicals found in food, In *Food Poisoning: Outbreaks, Bacterial Sources and Adverse Health Effects* (Ray, C. P., Ed.) pp 1-33, Nova Science Publishers, Hauppauge, New York.

(16) Griffin, C. T., Gosetto, F., Danaher, M., Sabatini, S., and Furey, A. (2014) Investigation of targeted pyrrolizidine alkaloids in traditional Chinese medicines and selected herbal teas sourced in Ireland using LC-ESI-MS/MS. *Food Addit Contam. Part A Chem. Anal. Control Expo. Risk Assess. 31*, 940-961.

(17) Schoental, R., Head, M. A., and Peacock, P. R. (1954) Senecio alkaloids: Primary liver tumours in rats as a result of treatment with (1) a mixture of alkaloids from *S. jacobaea lin*.; (2) retrorsine; (3) isatidine. *Br. J. Cancer 8*, 458-465.

(18) IARC. (2002) Some Traditional Herbal Medicines, Some Mycotoxins, Naphthalene and Styrene, In *IARC Monographs on the evaluation of carcinogenic risks of chemicals to humans* pp 153-168, International Agency for Research in Cancer, Lyon, France.

(19) IARC. (1976) Pyrrolizidine alkaloids, In *IARC Monograph on the evaluation of carcinogenic risk of chemicals to man - Some naturally occurring substance*, International Agency for Research in Cancer, Lyon, France.

(20) NTP. (2014) Riddelliine in *Report on Carcinogens 13th Edition National Toxicololgy Program* (Services, U. S. D. o. H. a. H., Ed.), Research Triangle Park, NC.

(21) Ruan, J., Yang, M., Fu, P., Ye, Y., and Lin, G. (2014) Metabolic activation of pyrrolizidine alkaloids: insights into the structural and enzymatic basis. *Chem. Res. Toxicol. 27*, 1030-1039.

(22) He, X., Xia, Q., and Fu, P. P. (2017) 7-Glutathione-pyrrole and 7-cysteine-pyrrole are potential carcinogenic metabolites of pyrrolizidine alkaloids. *J. Environ. Sci. Health, Part C 35*, 69-83.

(23) Xia, Q., Zhao, Y., Von Tungeln, L. S., Doerge, D. R., Lin, G., Cai, L., and Fu, P. P. (2013) Pyrrolizidine alkaloid-derived DNA adducts as a common biological biomarker of pyrrolizidine alkaloid-induced tumorigenicity. *Chem. Res. Toxicol. 26*, 1384-1396.

(24) Zhu, L., Xue, J., Xia, Q., Fu, P. P., and Lin, G. (2017) The long persistence of pyrrolizidine alkaloid-derived DNA adducts in vivo: kinetic study following single and multiple exposures in male ICR mice. *Arch. Toxicol. 91*, 949-965.

(25) Fu, P. P., Xia, Q., He, X., Barel, S., Edery, N., Beland, F. A., and Shimshoni, J. A. (2017) Detection of pyrrolizidine alkaloid DNA adducts in livers of cattle poisoned with heliotropium europaeum. *Chem. Res. Toxicol. 30*, 851-858.

(26) He, X., Ma, L., Xia, Q., and Fu, P. P. (2016) 7-N-Acetylcysteine-pyrrole conjugate—A potent DNA reactive metabolite of pyrrolizidine alkaloids. *J. Food Drug Anal. 24*, 682-694.

(27) He, X., Xia, Q., Ma, L., and Fu, P. P. (2016) 7-Cysteinyl-pyrrole conjugate-a new potential DNA reactive metabolite of pyrrolizidine alkaloids. *J. Environ. Sci. Health, Part C 34*, 57-76.

(28) Xia, Q., Ma, L., He, X., Cai, L., and Fu, P. P. (2015) 7-Glutathione pyrrole adduct: a potential DNA reactive metabolite of pyrrolizidine alkaloids. *Chem. Res. Toxicol. 28*, 615-620.

(29) Segall, H. J., Dallas, J. L., and Haddon, W. F. (1984) Two dihydropyrrolizine alkaloid metabolites isolated from mouse hepatic microsomes in vitro. *Drug Metab. Dispos. 12*, 68-71.

(30) Zhao, Y., Xia, Q., Gamboa da Costa, G., Yu, H., Cai, L., and Fu, P. P. (2012) Full structure assignments of pyrrolizidine alkaloid DNA adducts and mechanism of tumor initiation. *Chem. Res. Toxicol. 25*, 1985-1996.

(31) Yang, Y.-C., Yan, J., Doerge, D. R., Chan, P.-C., Fu, P. P., and Chou, M. W. (2001) Metabolic activation of the tumorigenic pyrrolizidine alkaloid, riddelliine, leading to DNA adduct formation in vivo. *Chem. Res. Toxicol. 14*, 101-109.

(32) Zhao, Y., Xia, Q., Yin, J. J., Lin, G., and Fu, P. P. (2011) Photoirradiation of dehydropyrrolizidine alkaloids-Formation of reactive oxygen species and induction of lipid peroxidation. *Toxicol. Lett. 205*, 302-309.

(33) Ma, L., Zhao, H., Xia, Q., Cai, L., and Fu, P. P. (2015) Synthesis and phototoxicity of isomeric 7, 9-diglutathione pyrrole adducts: Formation of reactive oxygen species and induction of lipid peroxidation. *J. Food Drug Anal. 23*, 577-586.

(34) Culvenor, C. C. J., Edgar, J. A., Smith, L. W., and Tweeddale, H. J. (1970) Dihydropyrrolizines III. Preparation and reactions of derivatives related to pyrrolizidine alkaloids. *Aust. J. Chem. 23*, 1853-1867.

(35) Mattocks, A. R., and Jukes, R. (1990) Recovery of the pyrrolic nucleus of pyrrolizidine alkaloid metabolites from sulphur conjugates in tissues and body fluids. *Chem. Biol. Interact. 75*, 225-239.

(36) Xia, Q., Zhao, Y., Lin, G., Beland, F. A., Cai, L., and Fu, P. P. (2016) Pyrrolizidine Alkaloid-Protein Adducts-Potential Non-Invasive Biomarkers of Pyrrolizidine Alkaloid-Induced Liver Toxicity and Exposure. *Chem. Res. Toxicol*. *29,* 1282-1292.

(37) Zhao, Y., Wang, S., Xia, Q., Gamboa da Costa, G., Doerge, D. R., Cai, L., and Fu, P. P. (2014) Reaction of dehydropyrrolizidine alkaloids with valine and hemoglobin. *Chem. Res. Toxicol. 27*, 1720-1731.

(38) Jiang, X., Wang, S., Zhao, Y., Xia, Q., Cai, L., Sun, X., and Fu, P. P. (2015) Absolute configuration, stability, and interconversion of 6, 7-dihydro-7-hydroxy-1-hydroxymethyl-5H-pyrrolizine valine adducts and their phenylthiohydantoin derivatives. *J. Food Drug Anal*. *23*, 318-326.

(39) Churchwell, M. I., Beland, F. A., and Doerge, D. R. (2006) Quantification of O^6-methyl and O^6-ethyl deoxyguanosine adducts in C57BL/6N/T$k^{+/-}$ mice using LC/MS/MS. *J. Chromat. B 844*, 60-66.

(40) Lame, M. W., Morin, D., Jones, A. D., Segall, H. J., and Wilson, D. W. (1990) Isolation and identification of a pyrrolic glutathione conjugate metabolite of the pyrrolizidine alkaloid monocrotaline. *Toxicol. Lett. 51*, 321-329.

(41) Lin, G., Cui, Y. Y., and Hawes, E. M. (1998) Microsomal formation of a pyrrolic alcohol glutathione conjugate of clivorine. Firm evidence for the formation of a pyrrolic metabolite of an otonecine-type pyrrolizidine alkaloid. *Drug Metab. Dispos. 26*, 181-184.

(42) Cooper, R. A., and Huxtable, R. J. (1996) A simple procedure for determining the aqueous half-lives of pyrrolic metabolites of pyrrolizidine alkaloids. *Toxicon 34*, 604-607.